Available online at www.sciencedirect.com
ScienceDirect
Journal of Controlled Release 120 (2007) 18–26
journal of controlled release
www.elsevier.com/locate/jconrel

Targeting cancer cells using PLGA nanoparticles surface modified with monoclonal antibody

Petra Kocbek, Nataša Obermajer, Mateja Cegnar, Janko Kos, Julijana Kristl *

University of Ljubljana, Faculty of Pharmacy, Aškerčeva 7, 1000 Ljubljana, Slovenia

Received 11 December 2006; accepted 15 March 2007
Available online 30 March 2007

Abstract

Targeting drugs to their sites of action is still a major challenge in pharmaceutical research. In this study, polylactic-co-glycolic acid (PLGA) immuno-nanoparticles were prepared for targeting invasive epithelial breast tumour cells. Monoclonal antibody (mAb) was used as a homing ligand and was attached to the nanoparticle surface either covalently or non-covalently. The presence of mAb on the nanoparticle surface, its stability and recognition properties were tested. Protein assay, surface plasmon resonance, flow cytometry and fluorescence-immunostaining confirmed the presence of mAb on nanoparticles in both cases. However, a binding assay using cell lysate revealed that the recognition properties were preserved only for nanoparticles with adsorbed mAb. These nanoparticles were more likely to be bound to the targeted cells than non-coated nanoparticles. Both types of nanoparticles entered the target MCF-10A neoT cells in mono-culture. In co-culture of MCF-10A neoT and Caco-2 cells immuno-nanoparticles were localized solely to MCF-10A neoT cells, whereas non-coated nanoparticles were distributed randomly. Immuno-nanoparticles entered only MCF-10A neoT cells, while non-coated nanoparticles were taken up by both cell types, indicating specific targeting of the immuno-nanoparticles. In conclusion, we demonstrate a method by which mAbs can be bound to nanoparticles without detriment to their targeting ability. Furthermore, the results show the effectiveness of the new carrier system for targeted delivery of small or large active substances into cells or tissues of interest.

Keywords: Nanoparticles; PLGA; Active targeting; Monoclonal antibody; Cell co-culture

1. Introduction

The field of therapeutics has seen an exponential growth in new molecular entities, ranging from low molecular weight drugs to macromolecules like proteins and genes. However, the ideal drug substance which interacts site-selectively with its molecular target at a therapeutically-relevant level has not yet been established, at least not in clinical practice. Some degree of site-selective delivery has been achieved only with "targeting homing drugs" that specifically recognize their pharmacological target [1]. An important impetus since 1975 has come from the development of monoclonal antibodies (mAb) and the exploitation of their targeting properties and hence therapeutic potential [2]. The specificity of delivery using nanoparticles was initially a coincidental property, active targeting has now become a central concept in therapeutic research. This concept has been developed into practical application with the construction of a variety of immuno-conjugates, also known as drug-attached antibodies (Abs) [3–7]. Certain mAbs have been shown to initiate specific signalling cascades, which can potentiate the therapeutic effect of the attached drug [8,9]. The latter has been confirmed for chemotherapeutic drugs and tumour-targeting antibodies [8]. However, the number of drug molecules that can be attached to an antibody molecule is usually the limiting factor for such a strategy, especially for low potency drug molecules [9,10]. For high potency drug molecules such as proteins, the coupling reaction could affect the pharmacological and immunological activities of the drug molecule, as well as the *in vivo* fate [11].

Nanoparticles with specific recognition ligands bound to the surface have a good potential for site-selective delivery, and

* Corresponding author. Tel.: +386 1 47 69 521; fax: +386 1 42 58 031.
E-mail address: julijana.kristl@ffa.uni-lj.si (J. Kristl).

0168-3659/$ - see front matter © 2007 Elsevier B.V. All rights reserved.
doi:10.1016/j.jconrel.2007.03.012

offer higher drug carrier capacity than bioconjugates, as well as improved specificity for drug targeting [12]. The carrier material used can additionally protect the drug from premature release and degradation [13,14]. Ligands attached to the surface can include any molecule that selectively recognizes and binds molecules on target cells [9,15]. Of the different targeting ligands, such as peptides, glycoproteins, carbohydrates and polymers, mAbs have been the most widely studied [8].

In our previous study we developed poly(lactic-co-glycolic acid) (PLGA) nanoparticles as a delivery system, and showed that they could be used to deliver a protein drug intracellularly more efficiently and faster than could be achieved with the free protein [16]. However, the formulated delivery system was not able to distinguish between different cells. We report here the preparation of PLGA nanoparticles designed specifically to target breast tumour cells. For this purpose we used a mAb recognizing the specific profile of the cytokeratins expressed by these cells. Covalent and non-covalent binding were both employed to attach mAb to the surface of pre-formed PLGA nanoparticles. The amount of mAb attached to the nanoparticle surface, the stability and recognition properties of the formulated systems were all characterized, as well as their ability to target and enter antigen-rich MCF-7 and MCF-10A neoT cells in mono-culture and, specifically, in co-culture with Caco-2 cells.

2. Materials and methods

2.1. Materials

Poly(lactic-co-glycolic acid) (PLGA), 50:50, Resomer RG™ 503H) was obtained from Boehringer (Ingelheim, Germany), polyvinyl alcohol (PVA, Mowiol™ 4–98) from Hoechst (Frankfurt, Germany), ethyl acetate from Merck (Darmstadt, Germany), EDC (1-ethyl-3-(3-dimethylaminopropyl)-carbodiimide) from Fluka Chemie AG (Switzerland), Alexa Fluor® 546-labelled goat anti-mouse immunoglobulin and Blue Cell Tracker from Molecular Probes (Carlsbad, CA, USA), bovine serum albumin (BSA) and fluorescein from Sigma (St. Louis, MO, USA) and Coomassie Plus reagent from Pierce (Rockford, IL, USA). All reagents were of analytical grade.

2.2. Monoclonal antibody preparation

The mAb was prepared against soluble membrane proteins of MCF-7 human invasive ductal breast carcinoma [17]. We isolated the mAb from mouse hybridoma cell lines using the standard method of Koehler and Milstein [2]. It was purified from hybridoma culture medium by affinity chromatography on protein G-Sepharose (Pharmacia, Uppsala, Sweden). The mAb recognizes cytokeratins expressed in breast epithelial cell lines and breast tumour cells (manuscript in preparation).

The mAb was labelled with Alexa Fluor® 546 dye following the procedure of the manufacturer (Molecular Probes, USA). Sodium bicarbonate was added to mAb solution and transferred to Alexa Fluor® 546 reactive dye for one hour. The labelled mAb was purified on the resin and stored at −20 °C.

2.3. Preparation of PLGA nanoparticles

The procedure used to prepare nanoparticles was similar to that reported previously [18]. BSA was incorporated in nanoparticles as a model protein. 400 μl of aqueous solution of BSA (10 mg/ml) was added to 2 ml of ethyl acetate containing 0.45 mg fluorescein and 100 mg PLGA and the mixture stirred at 7000 rpm (Homogeniser, Omni Labteh, Omni International Inc. Warrington, VA, USA) with simultaneous sonication (Ultrasonic bath: 500 W, 30 kHz, UZ 4P, Iskra, Sentjernej, Slovenia). After 2 min of emulsification, 8 ml of aqueous solution of PVA (5%, w/w) was added to the w/o emulsion to form a w/o/w double emulsion and stirred further for 5 min. To solidify the nanoparticles, the organic solvent was extracted by stirring the double emulsion with 200 ml of aqueous solution of 0.1% (w/w) PVA at 5000 rpm for 5 min. The resulting dispersion of nanoparticles was centrifuged at 15,000 rpm for 15 min (Ultracentrifuge Sorvall RC 5C plus, Maryland, USA), washed three times with purified water and freeze-dried (−57 °C, 0.090 mbar, 24 h) (Christ Beta 1–8 K, Germany).

2.4. Characterization of nanoparticles

2.4.1. Particle size and zeta potential analysis

Freeze-dried nanoparticles were dispersed in deionized water. Their mean particle diameter and the width of the particle distribution (polydispersity index) were determined by photon correlation spectroscopy using a Zetasizer 3000 (Malvern Instruments, Worcestershire, UK). The particle charge was quantified as zeta potential by laser Doppler anemometry using the Zetasizer 3000. All measurements were made in triplicate.

2.4.2. Surface morphology

The surface morphology of the formulated nanoparticles was visualized by scanning electron microscopy (SEM). Before observation, powdered samples of freeze-dried nanoparticles were fixed onto metallic studs with double-sided conductive tape (diameter 12 mm, Oxon, Oxford instruments, UK). A Supra 35 VP (Oberkochen, Zeiss, Germany) scanning electron microscope was used with an acceleration voltage of 1.00 kV and a secondary detector.

2.5. Formulation of immuno-nanoparticles

2.5.1. Adsorption

Nanoparticles were dispersed in PBS, pH 5.0, (0.6 mg/ml) and a 600 μl aliquot was mixed with 200 μl of a solution of mAb (2 mg/ml) and adjusted to the volume of 500 μl with phosphate buffer. mAb was adsorbed onto the nanoparticles at 4 °C for 24 h, then centrifuged at 10,000 rpm for 15 min (Eppendorf Centrifuge 5415) to separate immuno-nanoparticles from free mAb. The sediment was washed with PBS, pH 7.4, and re-dispersed in 500 μl of PBS, pH 7.4. The control was run the same way as the sample but PBS was used instead of mAb solution.

2.5.2. Covalent binding

For the covalent attachment of mAb onto the nanoparticle surface, EDC reagent was employed in this study. 4.5 μg of EDC was added to 360 μl of a mixture of 400 μg nanoparticles and 400 μg mAb. The molar ratio of EDC to mAb was approximately 8.8. The reaction mixture was stirred gently for 2 h at room temperature. Excess linking reagent and soluble by-products were separated by centrifugation at 13,200 rpm for 10 min, and the sediment was washed three times with 1 ml PBS, pH 7.4. Finally, immuno-nanoparticles were re-dispersed in 100 μl of PBS and protein content determined by Bradford assay. Two controls were run in the same way as the reaction mixture, one lacking EDC, the other EDC and mAb.

EDC is a convenient carbodiimide used to form a variety of chemical conjugates, provided one of the molecules contains a primary amine and the other a carboxylic group. EDC can react with a carboxylic acid group to form a highly reactive *O*-acylisourea intermediate. This active species can then react with a nucleophile such as a primary amine to form an amide bond. The advantage of EDC is its water solubility, allowing direct addition of the reagent to the reaction mixture without prior organic solvent dissolution and is therefore suitable for conjugating bioactive molecules. In our case EDC was used to conjugate the primary amine group of mAb with the free carboxylic end group of PLGA nanoparticles, forming a connecting amide bond. Excess reagent and the isourea formed as the by-product of the cross-linking reaction are both water-soluble and can easily be removed [19].

2.6. Determination of mAb on the surface of nanoparticles

The following methods were used to confirm the mAb on the nanoparticle surface:

2.6.1. Flow cytometry

A dispersion of nanoparticles with Alexa Fluor® 546 labelled mAb was introduced directly into a flow cytometer and analyzed using FACSCalibur (Becton Dickinson, Inc., USA). As a control, non-coated nanoparticles were analyzed.

2.6.2. Surface plasmon resonance

Interaction of mAb-modified nanoparticles with protein A was monitored using Biacore X system (BIAcore, Uppsala, Sweden). An SA sensor chip with pre-immobilized streptavidin (BR-1003-98 BIAcore) was used to immobilize biotinylated protein A at a flow rate of 1 μl/min for 10 min. The reference cell was blocked with biotin (10 μM, 10 min). The chip was then washed with 5 μl of 10 mM glycine buffer (pH 2.2) at a flow rate of 30 μl/min. Identical wash cycles were used to regenerate the chip between assays. mAb-modified or non-coated nanoparticles were dispersed in PBST buffer (PBS with 0.05% Tween 20; 0.475 mg/ml) and 5 μl was injected for each assay. All the steps were performed at 25 °C with a flow rate of 1 μl/min in 0.05% PBST running buffer.

2.6.3. Protein assay

The Bradford method with Coomassie dye was used. 300 μl of Coomassie Plus reagent was added to 10 μl of dispersion of nanoparticles, either mAb-coated or non-coated, and after 10 min of incubation, the absorbance was measured at 595 nm using a microplate reader (Tecan GENios, Switzerland). The results were compared to a standard curve of BSA solution in the concentration range from 10 μg/ml to 750 μg/ml.

2.6.4. Fluorescence microscopy

A secondary Ab, Alexa Fluor® 546-labelled goat anti-mouse immunoglobulin, was used to identify the presence of mAb on the surface of nanoparticles. mAb-modified nanoparticles were treated with 0.5 μl of secondary Ab at room temperature for 2 h. The volume ratio between solution of secondary Ab and dispersion of immuno-nanoparticles was 1:1000. Samples were centrifuged at 13,200 rpm for 15 min and washed twice with 1 ml PBS to eliminate the excess secondary Ab. After final washing, the sediment was re-dispersed in PBS at pH 7.4, and the fluorescence intensity of both fluorescent dyes (fluorescein: λ_{ex} 494 nm and λ_{em} 525 nm, and Alexa Fluor® 546: λ_{ex} 556 nm and λ_{em} 573 nm) was measured using a microplate reader (Safire^2 ™ Tecan, Switzerland). Furthermore, localization of both fluorescent dyes was observed with fluorescence microscopy using a Carl Zeiss LSM 510 confocal microscope. Alexa Fluor® 546 and fluorescein were excited with an argon (488 nm) or He/Ne (543 nm) laser and the emission was filtered using a narrow band LP 505–530 nm (green fluorescence) and 560 nm (red fluorescence) filter. Images were analyzed using Carl Zeiss LSM image software 3.0.

The stability of the complex of mAb adsorbed on nanoparticles labelled with secondary Ab was followed for 24 h in complete growth medium containing serum proteins and observed under the fluorescence microscope.

2.7. Cell cultures

MCF-7 and MCF-10A neoT cell lines originate from human breast epithelial cells. MCF-7 cells were obtained from American type culture collection (ATCC) (Rockville, Maryland, USA); MCF-10A neoT cells were provided by Prof. Bonnie F. Sloane (Wayne State University, Detroit, MI, USA). Cells were cultured in monolayers to 80% confluence in DMEM/F12 medium (1:1, v/v) supplemented with 2 mM glutamine, 10 μg/ml insulin, 0.5 μg/ml hydrocortisone, 20 ng/ml epidermal growth factor, HEPES, antibiotics and 5% fetal bovine serum at 37 °C in a humidified atmosphere containing 5% CO_2. For use in experiments 2.5×10^4 cells per well were seeded in a LabTek chambered coverglass system (Nalge Nunc International, Denmark) and allowed to attach for 24 h prior to the assay.

Caco-2 cells, originating from human colon adenocarcinoma cells, were obtained from ATCC. They were cultured to 80% confluence in MEM medium supplemented with 2 mM glutamine, 0.1 mM non-essential amino acids and 10% fetal bovine serum at 37 °C in a humidified atmosphere containing 5% CO_2.

To visualize the cells and distinguish between MCF-10A neoT cells and Caco-2 cells in co-culture, Caco-2 cells were stained using the fluorescent dye Blue Cell Tracker (10 μM) according to the manufacturer's protocol.

A co-culture of MCF-10A neoT cells and Caco-2 cells was prepared by seeding 2×10^4 Blue Cell Tracker labelled Caco-2 cells in a LabTek chambered coverglass system with 1×10^4 MCF-10A neoT cells and allowing to attach for 24 h prior to the targeting assay. The seeding ratio between MCF-10A neoT and Caco-2 cells was 2:1 due to the slower doubling time of the latter.

2.8. Recognition properties of immuno-nanoparticles

A preliminary test for binding ability of formulated immuno-nanoparticles was performed using MCF-7 or MCF-10A neoT cell lysates. Cells were trypsinized with 0.05% trypsin and 0.02% EDTA in PBS, pH 7.4, centrifuged and washed with PBS. 500 μl of lysis buffer (400 mM phosphate buffer, pH 6.0, 75 mM sodium chloride, 4 mM EDTA, 0.25% mM Triton X-100) was added. The lysate was frozen at −70 °C, melted, sonicated, and centrifuged for 15 min at 3300 rpm and 4 °C. The supernatant was diluted with carbonate buffer, pH 9.6, at a ratio of 1:5 and microtiter plates (Nunc-Immuno™ Break Apart™ Modules, Denmark) were coated by adding a 100 μl aliquot to each well and incubating at 4 °C for 24 h. Unoccupied sites were blocked using blocking buffer (3% BSA in PBS, pH 7.2), incubated at room temperature for half an hour and washed three times with washing buffer (PBS with 0.05% Tween 20, pH 7.2) (Washer, Dispenser Columbus, Tecan, Austria).

150 μl of immuno- or non-coated nanoparticles (0.375 mg/ml) was added to each pre-coated well, incubated 2 h at 37 °C and washed three times with PBS, pH 7.4 to remove unbound nanoparticles. Bound nanoparticles were hydrolysed with 150 μl of 1 M sodium hydroxide added to each well and the fluorescence of samples was measured using a microplate reader (Safire^2 ™ Tecan, Switzerland).

2.9. Cell targeting and internalization of immuno-nanoparticles

Cellular targeting and uptake of non-coated and immuno-nanoparticles were investigated with a mono-culture of MCF-10A neoT cells or a co-culture of MCF-10A neoT and Caco-2 cells. 100 μl of samples containing 0.5 mg nanoparticles/ml of growth medium were added to the cells and incubated at 37 °C for different time periods up to 24 h. The cells were then washed three times with growth medium to remove nanoparticles not internalized by the cells. Fluorescence microscopy was then performed using an Olympus IX/81 inverted fluorescence microscope equipped with a Dapi/FITC/TxRed filter set (E0435016) capable of distinguishing between the green (fluorescein in nanoparticles) and blue (Blue Cell Tracker staining of Caco-2 cells) fluorescence. Images were analyzed using Cell^R Imaging software.

Additionally, internalization of non-coated and immuno-nanoparticles into MCF-10A neoT cells was evaluated using flow cytometry. Cells were placed into twelve well plates (3×10^5/well) and left to attach. 200 μl of fluorescein-loaded immuno- or non-coated nanoparticles (0.3 mg/ml) were added to each well and incubated for 1, 4 or 24 h. As a control, cells were grown separately in the absence of nanoparticles. Flow cytometry was performed on a FACSCalibur (Becton Dickinson, Inc., USA).

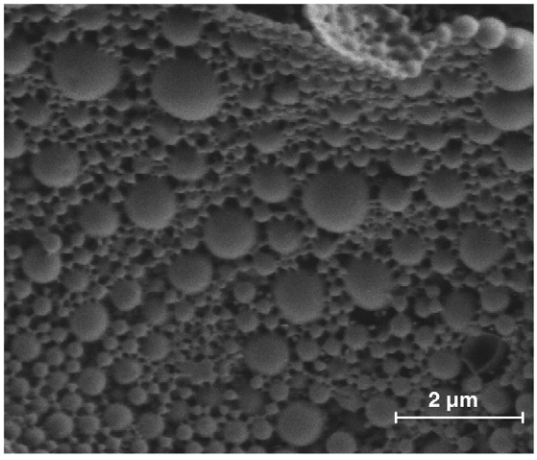

Fig. 1. SEM image of the PLGA nanoparticles.

3. Results

In order to achieve an immuno-nanoparticle system able to target desired cells, the binding procedure must preserve the biological activity of targeting ligand. In the present study a special focus was oriented to the selection of a suitable method for modification of the nanoparticle surface with mAb under aspect of an effective binding to particle surface and still preserving its biological activity. For this purpose mAb was bound to the surface of PLGA nanoparticles either by adsorption or covalent binding.

3.1. Nanoparticle preparation and characterization

Nanoparticles were prepared from a PLGA polymer containing free carboxylic end groups, using a modified double emulsion solvent diffusion method [18]. The resulting nanoparticles had a mean diameter of 320–360 nm, with a polydispersity index of 0.34. The mean zeta potential of nanoparticles was −25 mV, indicating that some free carboxylic end groups of the polymer were located on the surface of nanoparticles. The scanning electron micrograph images of the nanoparticles revealed their regular spherical shape, as well as a range of diameters (Fig. 1).

3.2. Determination of mAb on the surface of nanoparticles

The protein assay was used to quantify the amount of covalently bound mAb on nanoparticle surface. Since this assay cannot distinguish covalently bound mAb from adsorbed mAb or BSA in nanoparticles, two controls were run. The first one, evaluating the influence of adsorbed mAb, was run in the absence of EDC and the second, evaluating the contribution of non-coated nanoparticles, was run without EDC and mAb. The amount of mAb covalently bound to the nanoparticle surface was shown to be approximately 20 μg mAb per 1 mg of

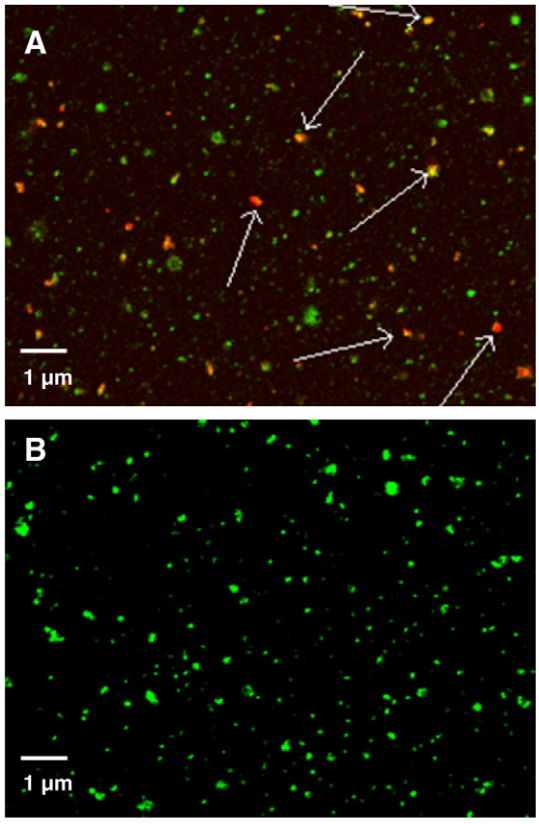

Fig. 2. Confocal microscopic images of fluorescein-loaded nanoparticles (green) with adsorbed mAb and Alexa Fluor® 546-labelled secondary antibody (red). White arrows indicate some of the nanoparticles coated with mAb (A). The control sample of nanoparticles (B) was incubated in the absence of mAb.

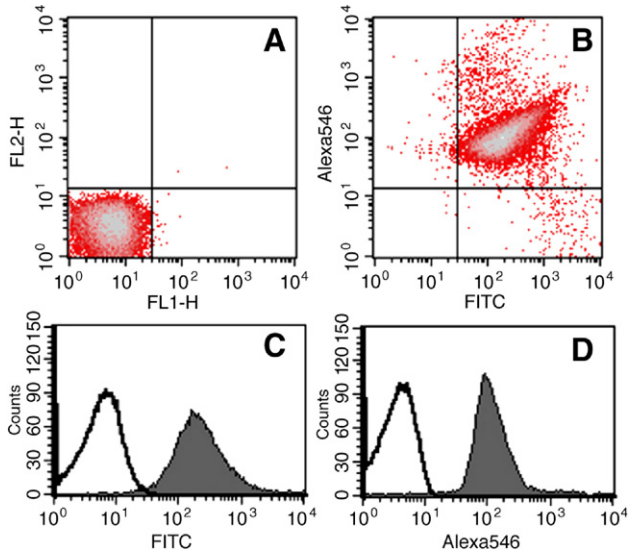

Fig. 3. Flow cytometry analysis of non-coated nanoparticles and fluorescein-loaded nanoparticles pre-incubated with mAb labelled with Alexa Fluor® 546. Density plots of non-coated nanoparticles (A) and mAb-coated nanoparticles (B) show that mAb-coated nanoparticles are homogenously coated with Alexa Fluor® 546-labeled mAb and can be distinguished from non-coated nanoparticles by their fluorescence. A shift of fluorescein (C) and Alexa Fluor® 546 (D) fluorescence intensity can be seen for immuno-nanoparticles (grey histograms) in comparison to non-coated nanoparticles (white histograms) indicating the presence of mAb on the surface of fluorescein-loaded nanoparticles.

nanoparticles. The protein content in covalently reacted sample was higher for 9% (w/w) regarding the first control and for 15% (w/w) regarding the second control. This demonstrated that mAb was covalently bound to the nanoparticle surface in the presence of EDC.

Non-covalent binding of mAb to the nanoparticle surface was evaluated first by fluorescence microscopy, using Alexa Fluor® 546 labelled secondary Ab recognizing mAb to visualize the adsorption of mAb on the surface of the fluorescein-loaded PLGA nanoparticles. Unlike the non-coated nanoparticles (Fig. 2B) the immuno-nanoparticles (Fig. 2A) show red fluorescence, indicating a certain proportion of nanoparticles with adsorbed mAb. The control (Fig. 2B) shows that the secondary Ab does not adsorb directly to the nanoparticle surface under the incubation conditions used (2 h). Additionally, results from flow cytometry showed that practically all nanoparticles are mAb coated and that the population of immuno-nanoparticles is rather homogenous (Fig. 3).

The extent of adsorption of mAb on the surface of nanoparticles was evaluated by measuring the fluorescence of the fluorescein in the nanoparticles and of Alexa Fluor® 546-labelled secondary Ab using a microtiter plate reader. The ratio of fluorescence intensities (Alexa Fluor® 546/fluorescein) was 0.565±0.008 for immuno-nanoparticles and 0.259±0.111 for non-coated nanoparticles. This indicated that a larger amount of secondary Ab was present on immuno-nanoparticles than on non-coated nanoparticles, confirming the presence of mAb on the immuno-nanoparticle surface. Surface plasmon resonance, with protein A (that binds specifically to the Fc region of immunoglobulin molecules [20]) immobilized on the sensor chip, showed a specific interaction of immuno-nanoparticles with protein A than non-coated nanoparticles, as is evident from the binding curves (Fig. 4).

The mAb-nanoparticle complex was shown, using fluorescence microscopy, to be stable in the presence of serum proteins (data not shown). Immunofluorescence images of double-labelled nanoparticles having adsorbed primary and secondary Ab showed discrete green and red coloured particles that persisted over a time period of 24 h.

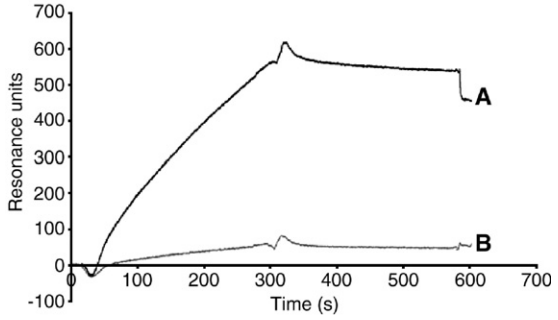

Fig. 4. Surface plasmon resonance analysis of immuno-nanoparticles (A) and non-coated nanoparticles (B) interaction with protein A immobilized on a sensor chip using BIAcore X system. The samples were injected over the protein A surface at a flow rate of 1 μl/min in 1% PBST running buffer at 25 °C.

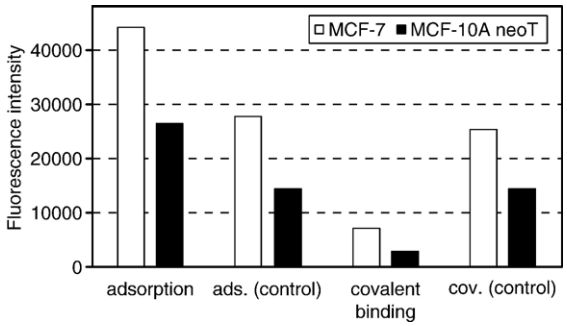

Fig. 5. Fluorescence intensity representing binding of nanoparticles, having either adsorbed or covalently bound mAb, to the antigen in MCF-7 and MCF-10A neoT cell lysates. The concentration of nanoparticles in each sample was kept constant (500 μg/ml). The controls represent non-coated nanoparticles in both cases.

3.3. Recognition properties of immuno-nanoparticles

Cell lysates were used to test the ability of mAb to bind to cell-type-specific antigens. Lysates were prepared from two invasive breast epithelial cell lines, MCF-7 and MCF-10A neoT. Nanoparticles with adsorbed mAb bind to the cell lysates and the extent of binding is approximately one third higher than that of the control, non-coated nanoparticles (Fig. 5). This indicates that the recognition properties of mAb did not change during the adsorption process. Although non-specific binding did take place, as is evident from the histogram for non-coated nanoparticles, mAb increased the level of binding, indicating the influence of the adsorbed mAb. On the other hand, covalent coupling of mAb on nanoparticles resulted in a significant loss of binding affinity to cytokeratins in cell lysates. Moreover, the binding of covalently-modified nanoparticles was even smaller than that of unmodified nanoparticles (Fig. 5). Greater association of immuno-nanoparticles was observed for MCF-7 cell lysate than for MCF-10A neoT lysate.

3.4. Cellular uptake of immuno-nanoparticles by MCF-10A neoT cells

The uptake of nanoparticles was evaluated by fluorescence microscopy and flow cytometry. Both methods confirmed internalization of non-coated and immuno-nanoparticles, although microscopy showed some delay for immuno-nanoparticles. On the micrograph images, internalized non-coated and

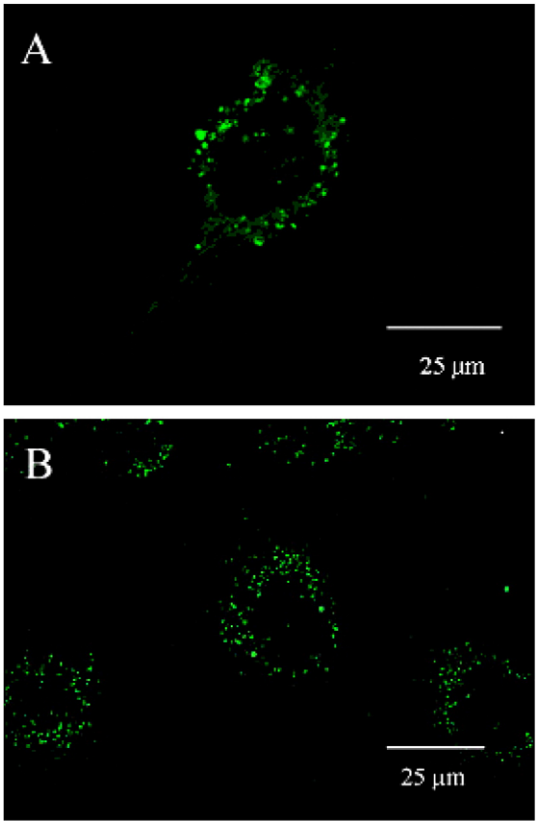

Fig. 6. Internalization of fluorescein-loaded PLGA nanoparticles coated with mAb (A) and non-coated nanoparticles (B) into MCF-10A neoT cells after 12 h of incubation. A perinuclear localization of internalized nanoparticles (green) was observed in both cases.

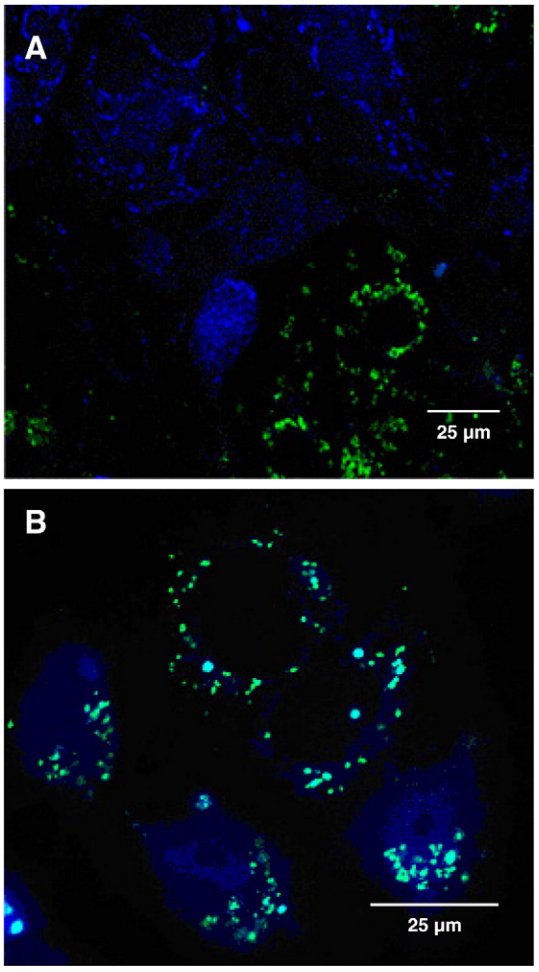

Fig. 7. Fluorescence microscope image of a co-culture of MCF-10A neoT and Caco-2 cells incubated with fluorescein-loaded PLGA nanoparticles coated with mAb (A) and uncoated nanoparticles (B) after 24 h of incubation. Immuno-nanoparticles (green) entered solely MCF-10A neoT cells, while non-coated nanoparticles entered both type of cells. The cells stained blue are Caco-2 cells.

immuno-nanoparticles were observed as green fluorescence spots, localized in the perinuclear region (Fig. 6). Flow cytometry analysis for both types of nanoparticles showed a shift in green fluorescence intensity due to internalization of fluorescein-loaded nanoparticles into MCF-10A neoT cells (data not shown). The uptake was detected after 1 h of incubation and increased progressively over the next 24 h. After 1 h 65% and 59% of cells had internalized immuno-nanoparticles and non-coated nanoparticles, respectively. After 4 h the fractions increased to 81% and 77%. Finally, after 24 h, 94% of cells internalized immuno-nanoparticles and 94% non-coated nanoparticles.

3.5. Cell targeting and internalization of immuno-nanoparticles in co-culture

The ability of immuno-nanoparticles in targeting MCF-10A neoT cells was evaluated in a co-culture with Caco-2 cells which lack the antigen for the mAb. Prior to internalization, immuno-nanoparticles localized in the vicinity of the MCF-10A neoT cells and not the Caco-2 cells, indicating their ability to target antigen-specific cells. By contrast, non-coated nanoparticles did not show such a specific localization towards MCF-10A neoT cells, as they were randomly distributed in the co-culture. Internalization of nanoparticles was checked after 24 h of incubation, and the uptake in MCF-10A neoT cell was observed only for nanoparticles having adsorbed mAb (Fig. 7).

4. Discussion

Drug targeting can improve the efficacy of therapy and reduce side effects associated with drugs [8,14]. Various carriers can be used to deliver a drug in a stable and protective form, however, it is nanotechnology which offers the most unique and intriguing approach in the area of nanomedicine [21,22].

In an attempt to formulate a carrier system for site-selective delivery, fluorescein-loaded PLGA nanoparticles capable of targeting invasive breast epithelial cell lines, such as MCF-7 and MCF-10A neoT, were developed. For this purpose we applied a mAb which recognizes the specific cytokeratin profile expressed by these cells. Two strategies for attaching mAb to nanoparticles were applied; covalent and non-covalent attachment. Nanoparticles with covalently bound mAb were prepared using EDC reagent. This reagent is frequently used for coupling reactions with bioactive molecules [19]. A linking spacer is usually used to bind mAb to nanoparticle surface, and only a few reports provide some data about direct coupling [12,23,24]. To investigate the possibility of direct coupling, no other reagent or linker was used in our study. By that strategy we achieved binding of mAb on nanoparticle surface, however, this attachment adversely affected the recognition properties of mAb for the target antigen. This could be due to the fact that proteins have numerous functional groups, therefore several side reactions can take place in the presence of EDC [19]. Carboxylic and amino groups are involved in covalent reaction with EDC reagent and both are present in mAb molecule, which may result in self-polymerization of mAb instead of coupling to nanoparticles. Such polymerized antibodies lose their specific recognition properties, making them inappropriate for drug targeting [19]. Moreover, amino groups within mAb antigen binding domains could be affected by covalent coupling, impairing its biological activity [11]. Direct covalent attachment of mAb on the nanoparticle surface could hinder the accessibility of the ligand as well. Furthermore, attached mAb, changed the surface properties of nanoparticles. Having the protein coating but lacking targetability, these nanoparticles exhibit more hydrophilic character and therefore interact more weakly with components of cell lysates as compared to non-coated hydrophobic PLGA nanoparticles, as observed in our study (Fig. 5). Direct covalent coupling was thus inappropriate to obtain effective immuno-nanoparticles in this study.

In the second method, nanoparticles were incubated with mAb to allow non-specific adsorption onto their surface, as reported by Illum et al. [25]. It has been suggested that hydrophobic interactions take part in this process, resulting from the attraction between the hydrophobic PLGA polymer and the non-polar (hydrophobic) part of the Ab molecule. Fluorescence microscopy, surface plasmon resonance, and flow cytometry confirmed the adsorption of mAb on the surface of nanoparticles. Flow cytometry showed that all nanoparticles were successfully coated with mAb, resulting in a homogenous population of immuno-nanoparticles. The adsorption is reversible and several authors emphasized the importance of competitive displacement of mAb that can take place in the presence of serum components [25–27]. However, our formulation, followed for 24 h in complete growth medium, was not influenced by the presence of serum proteins. Moreover, the pH of the incubation medium (pH 7.4), was close to the isoelectric point of the mAb used (p*I* 6.55–7.35) which favours the adsorption of protein on nanoparticle surface as suggested by Tsai et al. [28]. They investigated the adsorption of peptides to PLGA surface and asserted that this process is most favourable when the peptide is uncharged, thus less soluble, and exerts more hydrophobic character that interacts with the hydrophobic surface. Thus, the formulated nanoparticles with adsorbed mAb show promise as a suitable targeted delivery system.

The adsorbed mAb remained capable of targeting MCF-7 and MCF-10A neoT cells, recognizing the antigen expressed by these cells as observed by the cell lysate assay. Thus, the formulation procedure did not impair the native conformation of these biomolecules, as also documented by others [25]. Illum and coworkers reported that the orientation of Ab adsorbed on the surface of nanoparticles depends on the surface properties of the nanoparticles [25]. Antibody tends to bind to the hydrophobic surface through a constant region (Fc) of the molecule, leaving the antigen-binding sites free to interact with the antigen. PLGA is a hydrophobic polymer [29], thus it is most likely that mAb is adsorbed onto the nanoparticle surface via its Fc region, keeping antigen binding sites free to bind to the target antigen in the cell lysates. This binding was more specific for immuno-nanoparticles than for non-coated nanoparticles. On the other hand, surface plasmon resonance analysis showed that some mAb were adsorbed on the nanoparticle surface through antigen-binding domains, since Fc regions were free to interact with protein A immobilized on the sensor chip. The results thus suggest that the

orientation of adsorbed mAb on the nanoparticle surface is random.

The uptake of nanoparticles is influenced by nanoparticle shape, size, surface properties and concentration in the medium, incubation time and temperature, etc. [30–35]. The internalization studies using fluorescence microscopy showed that uptake of immuno-nanoparticles was slower than that of non-coated nanoparticles. This could be due to the hydrophilic surface resulting from the presence of mAb on nanoparticles as also suggested by other authors who observed decrease in the uptake by increasing hydrophilicity of nanoparticles [32]. However, flow cytometry did not show significant difference in the uptake of non-coated and immuno-nanoparticles.

Immuno-nanoparticles were observed to associate much more readily with the MCF-7 than with the MCF-10A neoT cell lysates. This is expected, since the anti-cytokeratin mAb used was prepared against MCF-7 cells. The binding was more specific for immuno-nanoparticles than for non-coated nanoparticles and dependent on the level of expression of the antigen.

In order to illustrate the cell specificity of the targeting of immuno-nanoparticles and non-coated nanoparticles, MCF-10A neoT and Caco-2 cells were grown in co-culture. This co-culture was set up specifically for such evaluation. The literature, however, usually deals only with experiments using one cell type when evaluating the uptake of targeted delivery system [12,23,24,25]. Using this experimental set up we were able to discriminate random and targeted nanoparticle internalization. Non-coated nanoparticles entered both cell types, while immuno-nanoparticles internalized only to the target MCF-10A neoT cells.

These experiments clearly indicate that antibodies, when attached to the nanoparticle surface in an active form, show the ability to target specific cells. Finally, nanoparticles localized to target cells can be employed to internalize and thus deliver cargo to intracellular recipients. However, it should be kept in mind that nanoparticles following the endocytotic pathway enter the lysosomal compartment, which can affect the formulation and/or the drug delivered by enzymic and chemical degradation. This particular method is thus suitable for lysosomal delivery, although certain polymeric carriers have the capability to escape the lysosomal compartment [36], allowing wider application of the strategy described here.

5. Conclusion

New PLGA nanoparticles, having the ability to recognize and target specific antigens on breast epithelial cancer cell lines, were prepared by attaching mAb on the nanoparticle surface via the adsorption process. Attempts to attach mAb to nanoparticles by covalent bonding were less successful, since the biological activity of the bound mAb was inactivated. The specificity of the immuno-nanoparticles was seen from their selective distribution in a co-culture of MCF-10A neoT and Caco-2 cells, resulting in their final internalization by the former cells.

Such modified nanoparticle delivery systems can provide suitable tools for effective targeted delivery of drugs into specific cells, especially in cases where the targets are localized intracellularly. A particularly valuable application would be in cancer therapy, since targeted delivery reduces side effects caused by unspecific drug uptake into healthy tissues. This approach would be appropriate for the delivery of various antitumour drugs ranging from small molecular weight drugs to large biomolecules, and offers the potential for much more effective antitumour therapy.

Acknowledgements

The authors thank Prof. Dr. Roger Pain for critical reading of the manuscript, Prof. Dr. Slavko Pečar for helpful discussion on covalent coupling, Urška Repnik from Institute Jožef Stefan, Department of Biochemistry, Molecular and Structural Biology, for assistance in flow cytometry, Mojca Lunder for assistance in surface plasmon resonance experiments, and Alenka Kužnik for isolation and characterization of mAb. This research work was supported by Ministry of Higher Education, Science and Technology of the Republic of Slovenia.

References

[1] K. Petrak, Essential properties of drug-targeting delivery systems, Drug Discov. Today 10 (23–24) (2005) 1667–1673.
[2] G. Kohler, C. Milstein, Continuous cultures of fused cells secreting antibody of predefined specificity, Nature 256 (5517) (1975) 495–497.
[3] M.C. Garnett, Targeted drug conjugates: principles and progress, Adv. Drug Del. Rev. 53 (2) (2001) 171–216.
[4] A. Funaro, A.L. Horenstein, P. Santoro, C. Cinti, A. Gregorini, F. Malavasi, Monoclonal antibodies and therapy of human cancers, Biotechnol. Adv. 18 (5) (2000) 385–401.
[5] P.A. Trail, A.B. Bianchi, Monoclonal antibody drug conjugates in the treatment of cancer, Curr. Opin. Immunol. 11 (5) (1999) 584–588.
[6] P.A. Trail, H.D. King, G.M. Dubowchik, Monoclonal antibody drug immunoconjugates, Cancer Immunol. Immunother. 52 (5) (2003) 328–337.
[7] J.M. Lambert, Drug-conjugated monoclonal antibodies for treatment of cancer, Curr. Opin. Pharmacol. 5 (5) (2005) 543–549.
[8] T.M. Fahmy, P.M. Fong, A. Goyal, W.M. Saltzman, Targeted for drug delivery, Mater. Today 8 (8) (2005) 18–26.
[9] P. Sapra, T.M. Allen, Ligand-targeted liposomal anticancer drug, Prog. Lipid Res. 42 (5) (2003) 439–462.
[10] S. Jaracz, J. Chen, L.V. Kuznetsova, I. Ojima, Recent advances in tumour-targeting anticancer drug conjugates, Bio. Med. Chem. 13 (17) (2005) 5043–5054.
[11] L. Nobs, F. Buchegger, R. Gurny, E. Allémann, Current methods for attaching targeting ligands to liposomes and nanoparticles, J. Pharm. Sci. 93 (8) (2004) 1980–1988.
[12] N. Dinauer, S. Balthasar, C. Weber, J. Kreuter, K. Langer, H. von Briesen, Selective targeting of antibody-conjugated nanoparticles to leucemic cells and primary T-lymphocytes, Biomaterials 26 (29) (2005) 5898–5906.
[13] J. Panyam, V. Labhasetwar, Biodegradable nanoparticles for drug and gene delivery to cells and tissue, Adv. Drug Del. Rev. 55 (3) (2003) 329–347.
[14] B. Stella, S. Arpicco, M.T. Peracchia, D. Desmaële, J. Hoebeke, M. Renoir, J. D'Angelo, L. Cattel, P. Couvreur, Design of folic acid-conjugated nanoparticles for drug targeting, J. Pharm. Sci. 89 (11) (2000) 1452–1464.
[15] J.K. Vasir, M.K. Reddy, V.D. Labhasetwar, Nanosystems in drug targeting: opportunities and challenges, Curr. Nanosci. 1 (1) (2005) 47–64.
[16] M. Cegnar, A. Premzl, V. Zavašnik - Bergant, J. Kristl, J. Kos, Poly (lactide-co-glicolide) nanoparticles as a carrier system for delivering cysteine protease inhibitor cystatin into tumor cells, Exp. Cell Res. 301 (2) (2004) 223–231.
[17] L. Beketic-Oreskovic, B. Sarcevic, B. Malenica, D.J. Novak, Immunocytochemical reactivity of a mouse monoclonal antibody CDI315B raised against human breast carcinoma, Neoplasma 40 (1993) 69.

[18] M. Cegnar, J. Kos, J. Kristl, Cystatin incorporated in poly(lactide-co-glycolide) nanoparticles: development and fundamental studies on preservation of its activity, Eur. J. Pharm. Sci. 22 (5) (2004) 357–364.
[19] G.T. Hermanson, Bioconjugate Techniques, I, Academic Press, London, 1996, pp. 169–172.
[20] H. Hjelm, K. Hjelm, J. Sjoquist, Protein A from *Staphylococcus aureus*. Its isolation by affinity chromatography and its use as an immunosorbent for isolation of immunoglobulins, FEBS Lett. 28 (1) (1972) 73–76.
[21] M. Cegnar, J. Kristl, J. Kos, Nanoscale polymer carriers to deliver chemotherapeutic agents to tumours, Exp. Opin. Biol. Ther. 5 (12) (2005) 1557–1569.
[22] L. Juillerat-Jeanneret, F. Schmitt, Chemical modification of therapeutic drugs or drug vector systems to achieve targeted therapy: looking for the grail, Med. Res. Rev. (in press).
[23] I. Steinhauser, B. Spänkuch, K. Strebhardt, K. Langer, Transtuzumab-modified nanoparticles: optimisation of preparation and uptake in cancer cells, Biomaterials 27 (28) (2006) 4975–4983.
[24] A. Cirstoiu-Hapca, L. Bossy-Nobs, F. Buchegger, R. Gurny, F. Delie, Differential tumor cell targeting of anti-HER2 Herceptin®) and anti-CD20 (Mabthera®) coupled nanoparticles, Int. J. Pharm. 331 (2) (2007) 190–196.
[25] L. Illum, P.D.E. Jones, J. Kreuter, R.W. Baldwin, S.S. Davis, Adsorption of monoclonal antibodies to polyhexylcyanoacrylate nanoparticles and subsequent immunospecific binding to tumour cells in vitro, Int. J. Pharm. 17 (1) (1983) 65–76.
[26] J. Barbet, P. Machy, L. Leserman, Monoclonal covalently coupled to liposomes: specific targeting to cells, J. Supramol. Struct. Cell. Biochem. 16 (3) (1981) 243–258.
[27] D. Leu, B. Manthey, J. Kreuter, P. Speiser, P.P. DeLuca, Distribution and elimination of coated polymethyl [2-^{14}C]methacrylate nanoparticles after intravenous injection in rats, J. Pharm. Sci. 73 (10) (1984) 1433–1437.
[28] T. Tsai, R.C. Mehta, P.P. DeLuca, Adsorption of peptides to poly(D,L-lactide-co-glycolide): 2. Effect of solution properties on the adsorption, Int. J. Pharm. 127 (1) (1996) 43–52.
[29] K.V. Roskos, R. Maskiewicz, in: L.M. Sanders, R.W. Hendren (Eds.), Degradable Controlled Release Systems Useful for Protein Delivery, Protein delivery: Physical Systems, vol. 10, Plenum Press, New York, 1997, pp. 45–92.
[30] V.P. Torchilin, Drug targeting, Eur. J. Pharm. Sci. 11 (Suppl. 2) (2000) S81–S91.
[31] J. Davda, V. Labhasetwar, Characterization of nanoparticle uptake by endothelial cells, Int. J. Pharm. 233 (1–2) (2002) 51–59.
[32] S.K. Sahoo, J. Panyam, S. Prabha, V. Labhasetwar, Residual polyvinyl alcohol associated with poly(D,L-lactide-co-glycolide) nanoparticles affects their physical properties and cellular uptake, J. Control. Release 82 (1) (2002) 105–114.
[33] J. Panyam, V. Labhasetwar, Dynamics of endocytosis and exocytosis of poly(D,L-lactide-co-glycolide) nanoparticles in vascular smooth muscle cells, Pharm. Res. 20 (2) (2003) 212–220.
[34] I. Lynch, Are there generic mechanisms governing interactions between nanoparticles and cells? Epitope mapping the outher layer of the protein–material interface, Physica, A Stat. Ther. Phys. 373 (2007) 511–520.
[35] R.E.S. Rowland, P.W. Taylor, A.T. Florence, Attachment, uptake and transport of nanoparticles coated with an internalin A fragment in Caco-2 cell monolayer, J. Drug Del. Sci. Technol. 15 (4) (2005) 313–317.
[36] J.S. Park, T.H. Han, K.Y. Lee, S.S. Han, J.J. Hwang, D.H. Moon, S.Y. Kim, Y.W. Cho, N-acetyl histidine-conjugated glycol chitosan self-assembled nanoparticles for intracytoplasmic delivery of drugs: endocytosis, exocytosis and drug release, J. Control. Release 115 (1) (2006) 37–45.